How long wavelengths can one extract from silica-core fibers?

Lægsgaard, Jesper; Tu, Haohua

Published in:
Optics Letters

Link to article, DOI:
10.1364/OL.38.004518

Publication date:
2013

Document Version
Publisher's PDF, also known as Version of record

How long wavelengths can one extract from silica-core fibers?

Jesper Lægsgaard[1,*] and Haohua Tu[2]

[1]*DTU Fotonik, Department of Photonics Engineering, Technical University of Denmark, Ørsteds Plads 343, DK-2800 Kongens Lyngby, Denmark*

[2]*Biophotonic Imaging Laboratory, University of Illinois at Urbana-Champaign, Urbana, Illinois 61801, USA*

**Corresponding author: jlag@fotonik.dtu.dk*

Received August 1, 2013; revised September 27, 2013; accepted October 1, 2013; posted October 2, 2013 (Doc. ID 195100); published October 31, 2013

The generation of wavelengths above 3 μm by nonlinear processes in short silica photonic crystal fibers is investigated numerically. It was found that wavelengths in the 3–3.5 μm range may be generated quite efficiently in centimeter-long fiber pieces when pumping with femtosecond pulses in the 1.55–2 μm range. Wavelengths in the range of 3.5–4 μm can in principle be generated, but these require shorter fiber lengths for efficient extraction. The results indicate that useful 3 μm sources may be fabricated with existing silica-based fiber technology. © 2013 Optical Society of America

OCIS codes: (060.2390) Fiber optics, infrared; (060.4370) Nonlinear optics, fibers; (060.5295) Photonic crystal fibers; (060.7140) Ultrafast processes in fibers; (190.5530) Pulse propagation and temporal solitons; (320.2250) Femtosecond phenomena.

http://dx.doi.org/10.1364/OL.38.004518

Fiber-based light sources for the mid-infrared wavelength range above 3 μm are of high interest because fiberized systems are expected to have advantages in robustness and ease of operation compared to solutions based on wavelength conversion in nonlinear crystals. A number of soft-glass material platforms are currently being investigated for this purpose [1]. Pure silica fibers, such as photonic crystal fibers (PCFs), seem less attractive in this wavelength range because of the strongly increasing losses beyond ~2–2.5 μm [2]. On the other hand, silica-based fiber technology has developed to a very mature state compared to most material alternatives, which allows for easy monolithic integration with silica-based fiber lasers [3]. It is therefore of interest to investigate how far this material platform can be pushed regarding mid-IR generation.

Conventional fiber-based supercontinuum sources that utilize picosecond pump pulses and fiber lengths of several meters rapidly lose spectral density at wavelengths beyond 2.3 μm [4]. Similarly, four-wave mixing based approaches suffer low conversion efficiencies to long wavelengths because of loss limitations [5,6]. Xia *et al.* demonstrated an extension of the supercontinuum edge toward 3 μm using 15 cm fiber pieces pumped with nanosecond 1.55 μm pulses [7]. In our work, the generation of long wavelengths from femtosecond (fs) pump pulses at wavelengths of 1.55 and 2 μm in still shorter fibers was studied numerically. PCFs with tailored dispersion properties served as the nonlinear medium. It is shown that existing silica PCF technology allows for the construction of sources in the 3–4 μm range provided one is able to work with sufficiently short fiber pieces.

The phenomenon of resonant energy transfer from solitons to dispersive waves in nonlinear fiber optics is well known [8], and the dispersive waves generated are often termed Cherenkov radiation (CR) because of formal analogies to Cherenkov radiation in one dimension. The intensity of the CR is controlled by the spectral density of the soliton at the CR frequency, ω_{CR}, which in turn is given by a phase matching condition whose linear (intensity-independent) part reads [8]

$$\tilde{\beta}(\omega_{\mathrm{CR}}) = \tilde{\beta}(\omega_p); \qquad \tilde{\beta}(\omega) = \beta(\omega) - \beta_1(\omega_p)(\omega - \omega_0). \quad (1)$$

Here, β is the frequency-dependent propagation constant of the fiber, $\beta_1 = d\beta/d\omega$ and ω_p is the center frequency of the 'pump' pulse. It is important to note that CR emission is not critically dependent on the presence of a stable soliton [9]. For instance, when intense fs pulses are coupled into optical fibers with anomalous dispersion, one initially observes strong spectral broadening by self-phase modulation (SPM), which in turn leads to dispersive pulse compression. With sufficient power, this process can generate a few-cycle pulse that rapidly breaks up into one or more fundamental solitons and residual dispersive waves around ω_p. However, around the point of maximal compression, one can observe strong transfer of optical power to CR frequencies fulfilling Eq. (1), and occurring over a mm or sub-mm length scale. Such rapid spectral conversion relaxes the constraints imposed by fiber loss, which is the basic idea behind the mid-IR generation scheme proposed here.

A standard PCF design, in which a triangular array of airholes make up the cladding region of the fiber, with one missing airhole defining the core, is capable of satisfying Eq. (1) over wide wavelength ranges with appropriate fiber parameters. This fact has been widely utilized for supercontinuum generation in the visible and near-IR wavelength regions [10]. Direct use of the CR mechanism for generating specific visible wavelengths from near-IR pump sources has also been demonstrated [3,11]. For PCFs having two zero-dispersion wavelengths, CR on the long-wavelength side of the soliton may be observed [1,12]. In Fig. 1, $\tilde{\beta}$ curves are shown for four fiber designs having $d/\Lambda = 0.8$, where d is the airhole diameter and Λ is the center-to-center distance between neighboring airholes. The curves were calculated by finding fully vectorial eigenmodes of Maxwell's equations with periodic

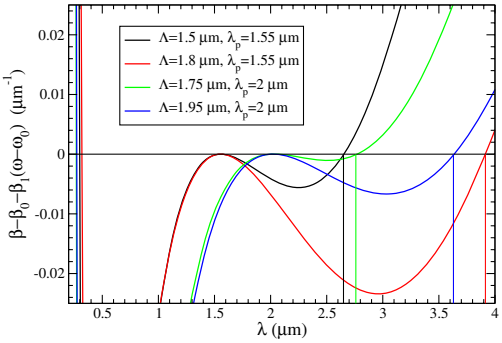

Fig. 1. $\tilde{\beta} - \beta(\omega_p)$ curves for a PCF with $d/\Lambda = 0.8$, and pump wavelengths λ_p characteristic of Er- or Tm-doped fiber lasers.

boundary conditions in a planewave basis using the freely available software package "MIT Photonic-Bands" [13]. Silica material dispersion was described by a perturbative scheme [14] using the Sellmeier parameters given by Okamoto [15]. These are very similar to the parameters found by Malitson [16] by fitting to refractive-index data ranging from 214 nm to 3.7 μm, thus providing some confidence in their use for the purposes of the present work. The pump wavelength was chosen to be either 1.55 or 2 μm, which is characteristic of either Er- or Tm-doped fiber lasers. The CR phase matching to wavelengths in the 3–4 μm range was readily obtained by scaling Λ in the range between 1.5–2 μm. There was also a phase matched ultraviolet (UV) CR frequency around 300 nm. Similar phase matching could also be obtained for lower d/Λ values. The high d/Λ value of 0.8 was chosen to ensure good confinement of the guided mode at the long CR wavelength.

The numerical simulations of nonlinear propagation were done using the generalized nonlinear Schrödinger equation (GNLSE) formulated in [17], although only nontapered fibers were considered here. The frequency integrals involved in the evaluation of the nonlinear operator were done over the full frequency axis i.e., no restriction to positive frequencies was done. This makes the formalism fairly general, the main approximations being the restriction to propagation in one polarization state of the fundamental mode. Restricting the integrations to positive frequencies was found to have a significant impact on the calculated spectra, although the qualitative predictions were similar. Frequency grids spanning wavelengths from 200–250 nm to 6 μm were employed to fully capture the effects of long- and short-wavelength CR as well as non-phase-matched third-harmonic generation (THG).

The main challenge for mid-IR generation is the silica material loss, so a reasonable model of the loss function is essential. In this work, the parametrization found by Frosz *et al.* was used [18,19]

$$\alpha = A_{\mathrm{UV}} e^{\lambda_{\mathrm{UV}}/\lambda} + A_{\mathrm{IR}} e^{-\lambda_{\mathrm{IR}}/\lambda}, \tag{2}$$

where $A_{\mathrm{UV}} = 10^{-3}$ dB/km, $A_{\mathrm{IR}} = 6 \cdot 10^{11}$ dB/km, $\lambda_{\mathrm{UV}} = 4.67$ μm, and $\lambda_{\mathrm{IR}} = 47.8$ μm. The IR constants were fitted to measurements in the 1.5–2.2 μm range. Loss curves for longer wavelengths have been reported by Izawa *et al.* [2]. The curve beyond 3 μm is bumpy and difficult to reproduce with a simple fit. Equation (2) compares reasonably with the experimental data, which include absorptions from a 30 ppm OH content, at 3 and 5 μm, while somewhat overestimating the losses in between. The predictions of the present paper should therefore be conservative. Note, however, that OH-induced absorptions will depend on the preparation and ambient conditions of the fiber. Also, confinement loss of the guided mode at the CR wavelength is not taken into account, since this can in principle be suppressed to any desired level by making the microstructured cladding sufficiently large.

Figure 2 shows simulated output spectra at wavelengths of 1.55 and 2.0 μm for fibers with different Λ-values when pumping with Gaussian pulses having 50 fs full width at half-maximum (FWHM). The input pulse energy was 4 nJ, which corresponds to a peak power of 75 kW. The propagation distance was set to 1 cm. The long CR wavelength was easily tuned in the 3–4 μm range by changing Λ. The conversion efficiency decreased strongly with increasing CR wavelengths mainly because of the attenuation rising from 0.7 dB/cm at 3 μm to ~40 dB/cm at 4 μm. As the main CR generation was found to occur within the first 2–4 mm of the fiber, the long-wavelength radiation was severely attenuated before the fiber exit.

The spectra in Fig. 2 also show peaks from nonresonant THG, and UV CR in the case of 1.55 μm pumping. The UV CR peak also appeared for 2 μm pumping at higher energies. It is undesirable for a long-wavelength source, since the presence of intense UV light is likely to degrade the fiber over time.

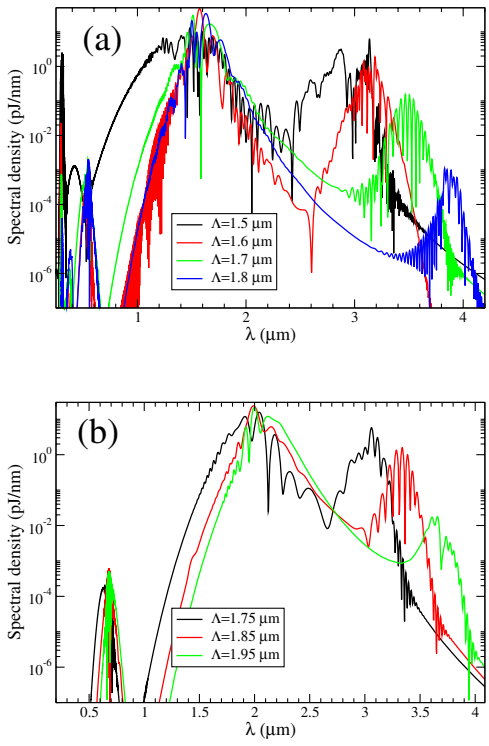

Fig. 2. Output spectra after 1 cm of propagation for a 4 nJ 50 fs input pulse at a wavelength of (a) 1.55 μm and (b) 2 μm. The PCF has $d/\Lambda = 0.8$.

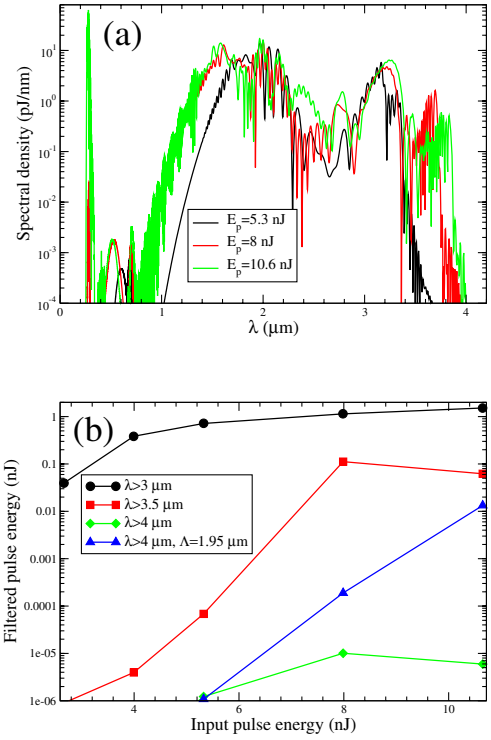

Fig. 3. (a) Output spectra after 1 cm propagation for a PCF with $\Lambda = 1.75$ μm, pumped by 50 fs pulses at 2 μm. (b) Long-pass filtered pulse energies versus input pulse energy for a fiber with $\Lambda = 1.75$ μm and one with $\Lambda = 1.95$ μm.

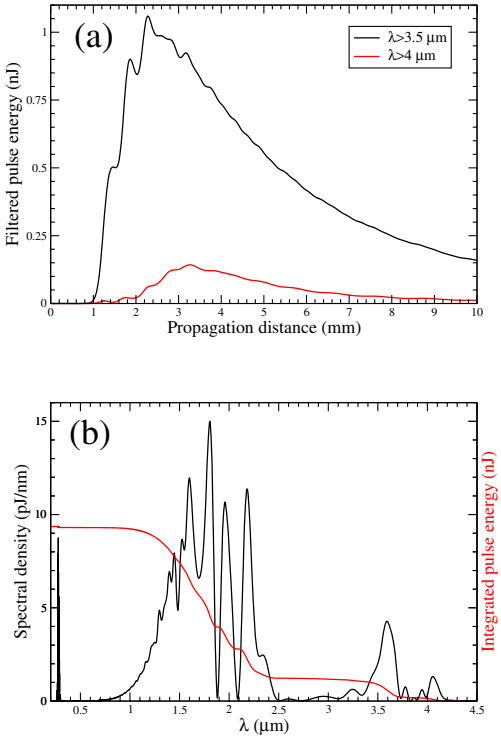

Fig. 4. (a) Long-pass filtered pulse energy versus propagation distance for a 10.6 nJ, 50 fs, Gaussian input pulse at 2 μm wavelength in a fiber with $\Lambda = 1.85$ μm. (b) Spectrum and cumulative integral after 3.3 mm propagation.

The conversion efficiency to the longer wavelengths can be increased by increasing the pump power. In Fig. 3, spectra for 2 μm pump pulses in a 1-cm PCF with $\Lambda = 1.75$ μm are shown at different pulse energies with fluences well below expected damage thresholds [20]. Also shown are the integrated pulse energy above cutoff wavelengths of 3, 3.5, and 4 μm. The energy above 3 μm reached 1.5 nJ for an input pulse energy of 10.6 nJ. However, above 3.5 μm, the maximal extracted energy was around 110 pJ, and it appeared at an input energy of 8 nJ. The decrease of the long-wavelength output energy with increasing pump power was due to the shift of the CR radiation toward longer wavelengths with correspondingly higher losses. Above 4 μm, the design with $\Lambda = 1.75$ μm delivered very little energy. Increasing Λ to 1.95 μm gave an output of 13 pJ for 10.6 nJ input energy, which still represents a very poor conversion factor.

The conversion efficiency to longer wavelengths may in principle be improved by further shortening of the fiber so that the desired long-wavelength radiation is generated just before the output facet. In this connection it should be noted that working with cm or sub-cm fiber pieces poses a substantial practical problem. In Fig. 4, the integrated energy beyond 3.5 and 4 μm for a 10.6 nJ input pulse is shown as a function of propagation distance for a fiber with $\Lambda = 1.85$ μm. The pulse energy above 3.5 μm peaks around 2.3 mm reaching a maximum of 1.06 nJ i.e., a 10% conversion efficiency. The energy beyond 4 μm reaches a maximum of 142 pJ after 3.3 mm. Given the assumption of ultrafast long-wavelength pump pulses and very short fiber lengths, these figures should be considered optimistic estimates of the conversion efficiencies obtainable in silica fibers. The spectrum after 3.3 mm is shown in the bottom panel of the figure along with the integrated (from the long-wavelength side) pulse energy. Note the appearance of the UV CR peak below 300 nm, which in this case carried around 50 pJ of energy.

The use of 50 fs input pulses improved conversion efficiency, but this is not a necessary requirement for generating long-wavelength CR. In Fig. 5, the spectrum of a 12.8 nJ input pulse with 300 fs FWHM is shown after 2 cm propagation in a fiber with $\Lambda = 1.75$ μm. The energy beyond 3 μm was 985 pJ, which corresponded to a conversion efficiency of 7.7%. Pulse breakup and CR generation initiates after about 1 cm propagation, a distance which decreases with increasing input power. Thus, the use of longer pulses relaxes the need for extremely short fiber pieces a bit. Although noise and shot-to-shot coherence was not modeled here, it must be expected that the use

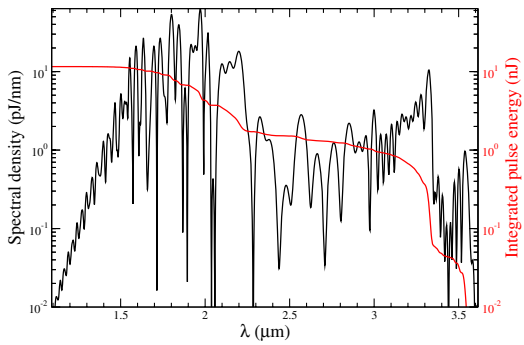

Fig. 5. Spectrum and its cumulative integral of a 300 fs 12.8 nJ input pulse after 2 cm propagation in a fiber with $\Lambda = 1.75$ μm.

of longer pulses will lead to a noisier CR signal in line with what one finds in fs-pumped continuum generation.

In summary, the generation of mid-IR light in the 3–4 μm wavelength range was shown to be feasible with existing silica-based PCFs. Accessing the 3.5–4 μm range in an efficient manner was found to require very short (sub-cm) fiber pieces, which represents a major practical challenge. On the other hand, wavelengths around 3 μm seem readily accessible with fiber lengths of a few cm, considering material losses on the order of 1 dB/cm. This wavelength range is of high interest for spectroscopy, imaging, and femtochemistry because of the presence of important fundamental stretching vibrations e.g., from O-H, N-H, and C-H chemical bonds.

The main limitations with the proposed generation scheme are the need to work with very short fiber pieces, the small core dimensions needed to obtain CR phase matching, which make power scaling difficult, and the possible appearance of unwanted UV radiation in the fiber. None of these issues are of a fundamental nature. Phase matching in larger cores without simultaneous phase matching to UV wavelengths might be obtained by more advanced fiber designs. The problem of working with short fiber lengths could possibly be avoided by chirping the input pulse and/or using tapered fibers. Research along these lines is currently in progress.

J. Lægsgaard acknowledges financial support by the Danish Council for Independent Research—Technology and Production Sciences (FTP). H. Tu acknowledges grant support from the National Institutes of Health (R01 CA166309).

References

1. J. H. V. Price, T. Monro, H. Ebendorff-Heidepriem, F. Poletti, P. Horak, V. Finazzi, J. Y. Y. Leong, P. Petropoulos, J. Flanagan, G. Brambilla, X. Feng, and D. Richardson, IEEE J. Sel. Top. Quantum Electron. **13**, 738 (2007).
2. T. Izawa, N. Shibata, and A. Takeda, Appl. Phys. Lett. **31**, 33 (1977).
3. X. Liu, J. Lægsgaard, U. Møller, H. Tu, S. A. Boppart, and D. Turchinovich, Opt. Lett. **37**, 2769 (2012).
4. U. Møller, S. T. Sørensen, C. Jakobsen, J. Johansen, P. M. Moselund, C. L. Thomsen, and O. Bang, Opt. Express **20**, 2851 (2012).
5. C. Jauregui, A. Steinmetz, J. Limpert, and A. Tünnermann, Opt. Express **20**, 24957 (2012).
6. A. Herzog, A. Shamir, and A. A. Ishaaya, Opt. Lett. **37**, 82 (2012).
7. C. Xia, M. Kumar, M.-Y. Cheng, O. P. Kulkarni, M. N. Islam, A. Galvanauskas, F. L. Terry, Jr., M. J. Freeman, D. A. Nolan, and W. A. Wood, IEEE J. Sel. Top. Quantum Electron. **13**, 789 (2007).
8. N. Akhmediev and M. Karlsson, Phys. Rev. A **51**, 2602 (1995).
9. K. E. Webb, Y. Q. Xu, M. Erkintalo, and S. G. Murdoch, Opt. Lett. **38**, 151 (2013).
10. J. M. Dudley, G. Genty, and S. Coen, Rev. Mod. Phys. **78**, 1135 (2006).
11. H. Tu and S. A. Boppart, Opt. Express **17**, 9858 (2009).
12. D. V. Skryabin, F. Luan, J. C. Knight, and P. S. J. Russell, Science **301**, 1705 (2003).
13. S. G. Johnson and J. D. Joannopoulos, Opt. Express **8**, 173 (2001).
14. J. Lægsgaard, A. Bjarklev, and S. E. B. Libori, J. Opt. Soc. Am. B **20**, 443 (2003).
15. K. Okamoto, *Fundamentals of Optical Waveguides* (Academic, 2000).
16. I. H. Malitson, J. Opt. Soc. Am. **55**, 1205 (1965).
17. J. Lægsgaard, J. Opt. Soc. Am. B **29**, 3183 (2012).
18. M. H. Frosz, P. M. Moselund, P. D. Rasmussen, C. L. Thomsen, and O. Bang, Opt. Express **16**, 21076 (2008).
19. S. T. Sørensen, "Deep-blue supercontinuum light sources based on tapered photonic crystal fibers," Ph.D. dissertation (Technical University of Denmark, 2013).
20. R. Cherif, M. Zghal, I. Nikolov, and M. Danailov, Opt. Commun. **283**, 4378 (2010).